

# Alternative Splicing Determines the Intracellular Localization of the Novel Nuclear Protein Nop30 and Its Interaction with the Splicing Factor SRp30c\*

(Received for publication, May 18, 1998, and in revised form, December 28, 1998)

Oliver Stoss, Franz-Werner Schwaiger, Thomas A. Cooper‡, and Stefan Stamm§

From the Max-Planck Institute of Neurobiology, Am Klopferspitz 18a, D-82152 Martinsried, Germany and the

‡Departments of Pathology and Cell Biology, Baylor College of Medicine, Houston, Texas 77030

**We report on the molecular cloning of a novel human cDNA by its interaction with the splicing factor SRp30c in a yeast two-hybrid screen. This cDNA is predominantly expressed in muscle and encodes a protein that is present in the nucleoplasm and concentrated in nucleoli. It was therefore termed Nop30 (nucleolar protein of 30 kDa). We have also identified a related cDNA with a different carboxyl terminus. Sequencing of the *NOP* gene demonstrated that both cDNAs are generated by alternative 5' splice site usage from a single gene that consists of four exons, spans at least 1800 nucleotides, and is located on chromosome 16q21-q23. The alternative 5' splice site usage introduces a frameshift creating two different carboxyl termini. The carboxyl terminus of Nop30 is rich in serines and arginines and has been found to target the protein into the nucleus, whereas its isoform is characterized by proline/glutamic acid dipeptides in its carboxyl terminus and is predominantly found in the cytosol. Interaction studies in yeast, *in vitro* protein interaction assays, and co-immunoprecipitations demonstrated that Nop30 multimerizes and binds to the RS domain of SRp30c but not to other splicing factors tested. Overexpression of Nop30 changes alternative exon usage in preprotachykinin and SRp20 reporter genes, suggesting that Nop30 influences alternative splice site selection *in vivo*.**

splicing (2, 3). Using the family member SRp30c (4) as an interactor in a two-hybrid screen, we have previously shown that the matrix attachment region element-binding protein SAF-B has the potential to link matrix attachment region elements, RNA polymerase II, and SR proteins (5). This supports growing evidence that gene expression achieved through RNA biosynthesis, RNA processing, and RNA transport is a highly coordinated process mediated by a network of proteins that has been termed the RNA "factory" (6) or transcriptosomal complex (7). For example, it has been shown that the carboxyl-terminal domain of RNA polymerase II binds to proteins involved in pre-mRNA processing (8, 9) and that 3' processing of pre-mRNA is coupled to components of the splicing machinery (6).

RNA processing is not just confined to polymerase II transcripts, since rRNA generated by polymerase I undergoes maturation that removes externally and internally transcribed spacers in various steps to yield 28S, 18S, and 5.8S ribosomal RNA in mammalian cells (10). This process is confined to nucleoli, the sites of ribosome biosynthesis. Three morphologically distinct areas of the nucleolus can be distinguished: the nucleolar fibrillar center, the dense fibrillar region, and the granular region. Functional studies have indicated that the fibrillar center is the region where ribosomal RNA genes, RNA polymerase I, and transcription factors are localized. The dense fibrillar region consists of unprocessed nascent ribosomal RNA and associated proteins. Mature 18S and 28S rRNA together with intermediates in ribosome assembly are found in the granular region. Thus, the morphological and functional compartmentalization of the nucleolus reflects specialized areas involved in rRNA synthesis, processing, and export (11, 12).

We are currently using yeast two-hybrid screens to identify novel proteins involved in RNA processing. Employing the splicing factor SRp30c (4) as a bait to screen a human library, we identified a cDNA coding for a nuclear protein that is enriched in nucleoli and migrates around 30 kDa on SDS-polyacrylamide gel electrophoresis. We therefore termed this protein Nop30. We identified an isoform of Nop30, which we call Myp. Myp has been previously isolated from rats in a screen aimed to find genes induced by nerve growth factor (13). Analysis of the *NOP* gene revealed that both isoforms are generated by alternative splicing. In contrast to the nuclear localization of Nop30, its isoform Myp is found in the cytosol. Overexpression of Nop30 with a cotransfected SRp20 or preprotachykinin minigene (14) affects splicing of the corresponding alternative exons in the reporter genes, suggesting a potential role of Nop30 in pre-mRNA splicing. Since Nop30 binds specifically to SRp30c and its mRNA is highly expressed in muscle, we suggest that this protein acts as a regulator of SR protein function in muscle.

In eukaryotes, gene expression is controlled at several levels. Due to the presence of cell-specific factors, genes can be transcribed in a cell type or developmentally regulated manner. Moreover, primary transcripts undergo maturation processes such as pre-mRNA splicing (1) and capping. A growing number of proteins containing an N-terminal RNA recognition motif and C-terminal clusters of serines and arginines (SR proteins)<sup>1</sup> have been shown to be involved in constitutive and alternative

\* This work was supported by the Max Planck Society, Human Frontier Science Program Grant RG562/96 (to S. S.), and National Institutes of Health Grant HL45565 (to T. A. C.). The costs of publication of this article were defrayed in part by the payment of page charges. This article must therefore be hereby marked "advertisement" in accordance with 18 U.S.C. Section 1734 solely to indicate this fact.

The nucleotide sequence(s) reported in this paper has been submitted to the GenBank™/EBI Data Bank with accession number(s) AF064598, AF064599, and AF064600.

§ To whom correspondence should be addressed. Tel.: 49 89 8578 3625; Fax: 49 89 8578 3749; E-mail: stamm@pop1.biochem.mpg.de.

<sup>1</sup> The abbreviations used are: SR proteins, serine/arginine-rich proteins; PPT, preprotachykinin; DiQ, 4-(4-(dihexadecylamino)styryl)-N-methylquinolinium iodide; PCR, polymerase chain reaction; RT-PCR, reverse transcription-PCR; GST, glutathione S-transferase; kb, kilobase pair(s); BHK, baby hamster kidney; EGFP, enhanced green fluorescent protein.

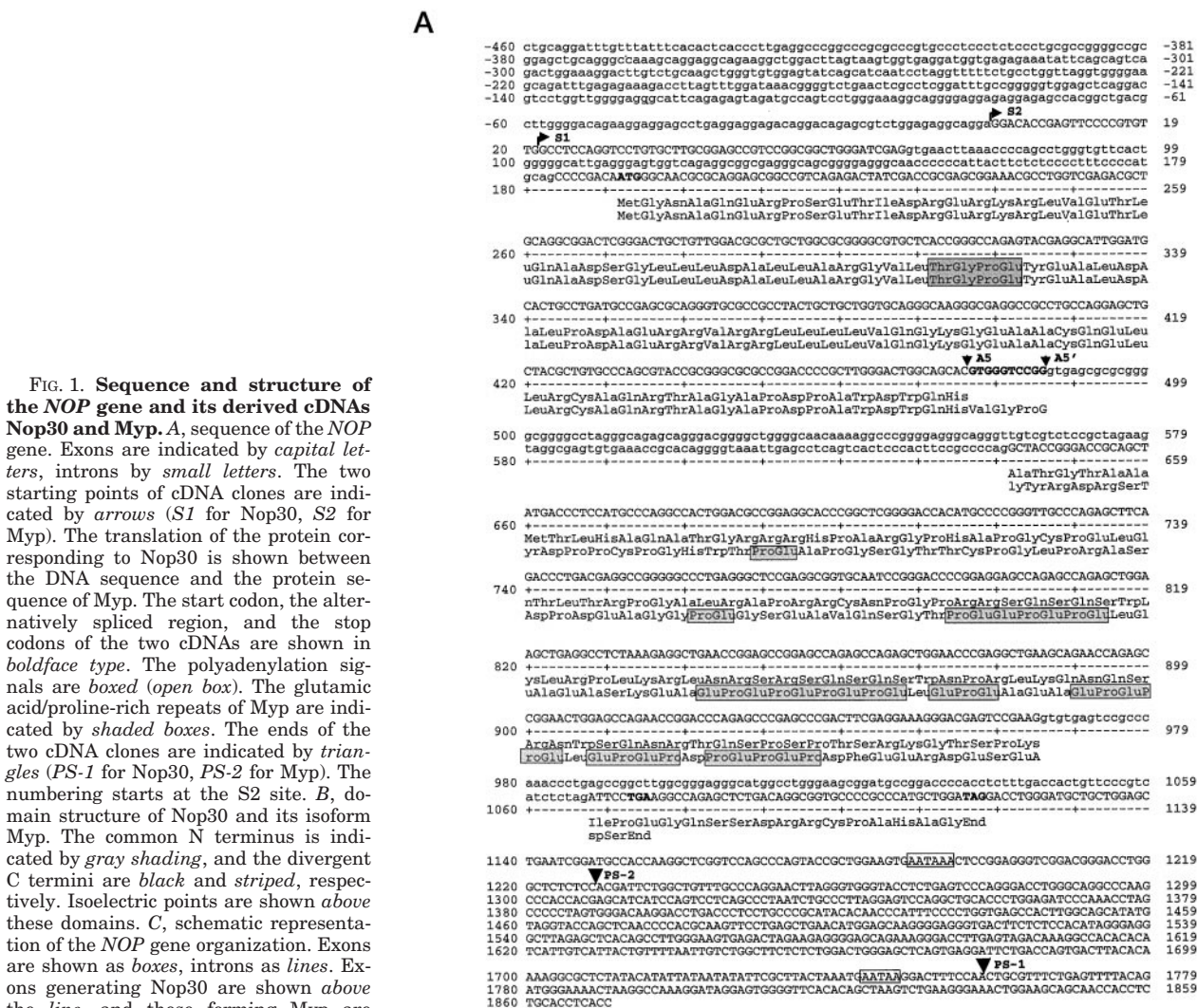
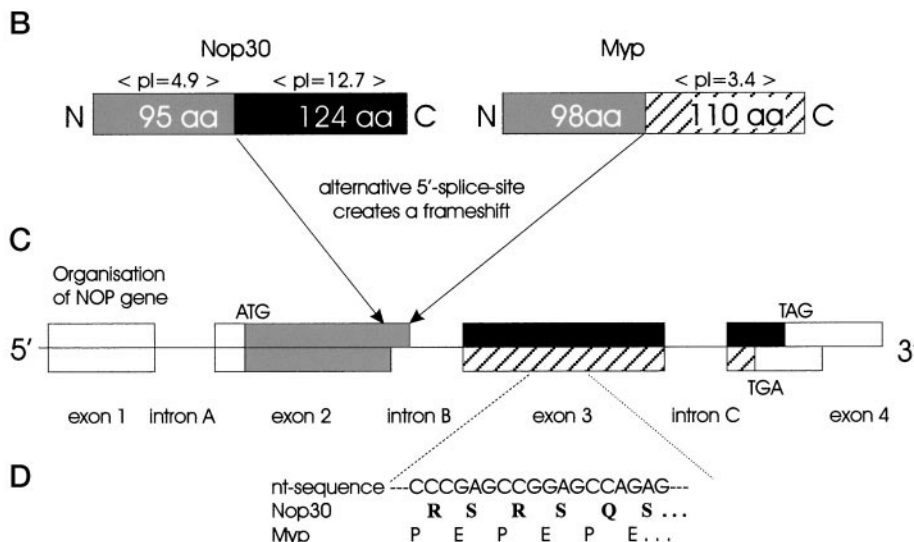


**FIG. 1. Sequence and structure of the NOP gene and its derived cDNAs Nop30 and Myp.** *A*, sequence of the NOP gene. Exons are indicated by capital letters, introns by small letters. The two starting points of cDNA clones are indicated by arrows (*S1* for Nop30, *S2* for Myp). The translation of the protein corresponding to Nop30 is shown between the DNA sequence and the protein sequence of Myp. The start codon, the alternatively spliced region, and the stop codons of the two cDNAs are shown in boldface type. The polyadenylation signals are boxed (open box). The glutamic acid/proline-rich repeats of Myp are indicated by shaded boxes. The ends of the two cDNA clones are indicated by triangles (*PS-1* for Nop30, *PS-2* for Myp). The numbering starts at the *S2* site. *B*, domain structure of Nop30 and its isoform Myp. The common N terminus is indicated by gray shading, and the divergent C termini are black and striped, respectively. Isoelectric points are shown above these domains. *C*, schematic representation of the NOP gene organization. Exons are shown as boxes, introns as lines. Exons generating Nop30 are shown above the line, and those forming Myp are shown below the line. Coding regions are indicated by shading. Different shading indicates differences resulting from the frameshift introduced by the alternative 5' splice site. *D*, change of the amino acid composition in the C terminus caused by alternative 5' splice site usage. aa, amino acids.



EXPERIMENTAL PROCEDURES

**Two-hybrid Screening**—A yeast two-hybrid screen using SRp30c as a bait in pGBT9 and a HeLa library was performed as described by Fields and Song (15). DNA from the autotrophic bacteria was sequenced using an ABI sequencer and analyzed with the GCG Wisconsin package (16). To test the interaction between proteins, 1 μg of a prey construct fused to the Gal4 activation domain in pADGal4 and 1 μg of bait-construct fused to the Gal4 binding domain were simultaneously co-transformed

and plated onto double dropout plates lacking leucine and tryptophan. Surviving colonies were restreaked onto triple dropout plates lacking leucine, tryptophan, and histidine and onto triple dropout plates supplemented with 5 and 10 mM 3-aminotriazole (Sigma).

**Genomic Cloning**—Using the cDNA of Nop30 as a probe, a human BAC library was screened (kindly performed by the German Human Genome Project). Two *PstI* fragments containing the complete clone were subcloned in pBluescript-SK(+) (Stratagene), and positive clones

were identified by colony hybridization (17).

**Computer Analysis**—Calculation of splice site scores was as described by Stamm *et al.* (18).<sup>2</sup>

**Chromosomal Localization**—Chromosomal localization was performed with the Stanford radiation hybrid panel 4.0 (Research Genetics Inc.). For PCR, the following primers were used: PEintrof1 (5'-GGTC-CGGGTGAGCGCGCGGG-3'; located in intron B) and PEint1 (5'-GAGATGACGGGAACAGTGGTCAAAG-3'; located in intron C). For data processing and mapping, World Wide Web servers were used.<sup>3</sup>

**Northern Blot**—Nop30 full-length cDNA, SRp30c cDNA, and a  $\beta$ -actin probe (CLONTECH) were labeled with radioactive [ $\gamma$ -<sup>32</sup>P]dCTP using the megaprime DNA labeling system from Amersham Pharmacia Biotech. A human multiple tissue Northern blot (CLONTECH) was probed according to the manufacturer's instructions.

**In Situ Hybridization**—0.2 ng of the cloned Nop30 probe was PCR-amplified using primers specific for Nop30 anchored by either the T7 or Sp6 RNA polymerase recognition sequence and purified using QiaQuick (Qiagen). Transcription using either T7 or Sp6 RNA polymerase was done according to the manufacturer's protocol (Boehringer Mannheim) using 250 ng of the respective PCR product as template. *In situ* hybridization histochemistry and the following washing steps were performed as described earlier (19). 20- $\mu$ m-thick dried cryostat sections were incubated with  $2 \times 10^6$  cpm of the [<sup>35</sup>S]UTP (Amersham Pharmacia Biotech)-labeled probe. After the washing steps, sections were dehydrated through graded ethanols containing 0.3 M ammonium acetate, air-dried, covered with a thin sheet of film emulsion (NBT-2, Eastman Kodak Co.), and exposed at 4 °C for 7 days. They were developed in Kodak D19 developer and fixed in 24% sodium thiosulfate. Sections were counterstained with Cresyl Violet, dehydrated, and mounted in DePeX (Gurr).

**Cloning of Deletion Variants**—The following constructs were generated with the primers indicated using PCR: EGFP-Nop30 $\Delta$ N with PEC (5'-GGCCATGAATTCACCATGGCTACCGGGACCGCAGTATG-3') and PEOBam (5'-GGCCATGGATCCCTATCCAGCATGGGCGGGCA-C-3'); Nop30 $\Delta$ C with PEOeco (5'-GGCCATGAATTCATGGGCAACGC-GCAGGAGCGG-3') and PEN (5'-GGCCATGGATCCTCAGTGCTGCC-AGTCCCAAGCGGG-3'); Myp $\Delta$ N with est1b (5'-GGCCATGAATTCGT-GGGTCCGGGTACCGGGAC-3') and est1c (5'-GGCCATGGATCCCT-ATCCAGCATGGGCGGGGAC-3'); 30c $\Delta$ RS with 30cdelr (5'-GGCCA-TGGATCCCTCAGGATAAACTCGGATGTAGG-3') and 30cdelf (5'-GGCCATGAATTCATGTCCGGGCTGGGCGGACGAG-3').

**Immunocytochemistry/DiQ Staining**—HEK293, BHK, or HeLa cells were grown on glass coverslips and transfected with 0.5  $\mu$ g of an EGFP fusion construct (in pEGFP-C2; CLONTECH), using the method of Chen and Okayama (20). The following EGFP fusion proteins were used: Nop30, Nop30 $\Delta$ N, Nop30 $\Delta$ C, Myp, Myp $\Delta$ N, SRp30c, and SRp30c $\Delta$ RS. Cells were cultured in Dulbecco's modified Eagle medium (Life Technologies, Inc.) supplied with 10% fetal calf serum (Life Technologies) for 18–24 h in 5% CO<sub>2</sub>. To counterstain cells, DiQ (4-(4-(dihexadecylamino)styryl)-N-methylquinolinium iodide; Molecular Probes, Inc., Eugene, OR) was added, followed by another 2 h of incubation. DiQ is a long-chain dialkylcarbocyanine that stains membranes and components of the cytoplasm, excluding the nucleus. Immunocytochemistry was performed as described (21). The following antibodies in phosphate-buffered saline, 0.1% Triton were used: a monoclonal anti-nucleolus antibody (1:300; Calbiochem), a polyclonal rabbit anti-FLAG antibody (1:150; Santa Cruz Biotechnology, Inc., Santa Cruz, CA), and a monoclonal B23 antibody (1:100; Ref. 22). For B23 staining, cells were permeabilized for 1 min with 100% acetone at -20 °C. After washing three times, the cells were incubated for 1 h with the appropriate antibody linked to Cy3 (1:500 in phosphate-buffered saline, 1% Triton). The cells were mounted using Gelmount (Biomed) and analyzed by confocal microscopy (Leica).

**Pull Down**—Nop30 was cloned in pCR3.1 (Invitrogen) and used for an *in vitro* reticulocyte lysate transcription/translation (TNT, coupled reticulocyte lysate system; Promega) to obtain <sup>35</sup>S-labeled Nop30 protein. For the binding experiments, glutathione-Sepharose 4B (Amersham Pharmacia Biotech) was washed three times with HNTG buffer (50 mM HEPES, pH 7.5, 150 mM NaCl, 1 mM EDTA, 10% glycerol, and 0.1% Triton X-100), (23), followed by incubation with 1  $\mu$ g of GST-SRp30c, GST-ASF/SF2, or GST; 10  $\mu$ l of glutathione-Sepharose 4B; 20

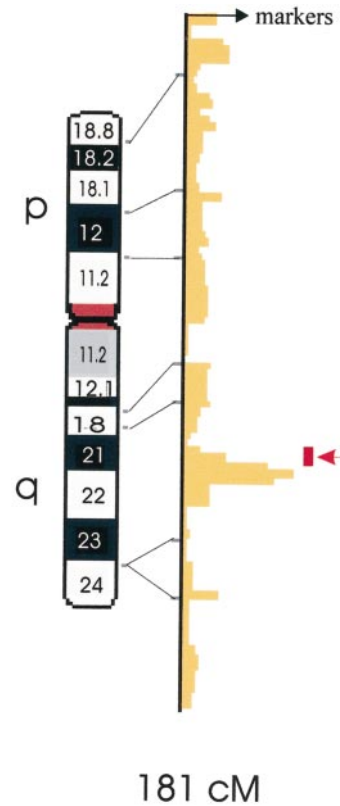


FIG. 2. Chromosomal localization of the *NOP* gene. Cytogenetic (left) and radiation hybrid map (right) of chromosome 16. *NOP* maps 3.15 cR from WI-5594, which corresponds to a region between 16q21 and 16q23. The most likely location on the radiation map of chromosome 16 is indicated by an arrow.

$\mu$ l of HNTG buffer; and 23,000 cpm of <sup>35</sup>S-labeled Nop30 with agitation overnight at 4 °C. After centrifugation, the supernatant was removed, and the pellet was washed three times with 500  $\mu$ l of HNTG buffer supplemented with 0.1% Triton X-100 and loaded onto a 12% SDS-polyacrylamide gel. Exposure of dried gels was made overnight on FujiX BAS 1000 phosphor imager plates.

**Immunoprecipitation and Western Blot**—For immunoprecipitation, human embryonic kidney (HEK) 293 cells were grown to 50% confluency and transfected with 0.1- $\mu$ g DNA constructs as indicated. Immunoprecipitation of the EGFP constructs was performed using an anti-GFP antibody (Boehringer Mannheim) (5). The co-precipitating FLAG constructs were analyzed after 10–15% SDS-polyacrylamide electrophoresis and Western blotting using an anti-FLAG antibody (Santa Cruz Biotechnology). SDS-polyacrylamide gel electrophoresis was performed as described by Laemmli (24), and protein was transferred onto ECL membranes (Amersham Pharmacia Biotech). Blocking of the membranes and protein detection was performed as described by Nayler *et al.* (23).

**Splicing Assays**—Transient transfection and RT-PCR was performed as described previously (5). The indicated amounts of pNop30-C2, pEGFP-C2 (CLONTECH) and pCG35 were co-transfected with 2  $\mu$ g of either the SRp20 (14) or PPT minigene in HEK293 cells or in fibroblasts, respectively. The next day, the transfection rate was assessed by fluorescence microscopy, and RNA was isolated from equally transfected cultures using the RNeasy Kit (Qiagen). For the SRp20 minigene, 30 cycles were used with annealing and extension temperatures of 55 and 72 °C with the primer pair T7 (5'-TAATACGACTCACTATAGGG-3') and X16R (5'-CCTGGTCGACACTCTAGATTTCTTTCATTGAC-3'). PCR products were resolved on a 1.5% agarose gel, stained with ethidium bromide, and quantified using the Herolab EASY system. For the PPT minigene, reverse transcription followed by radioactive PCR using the primers T7PRO (5'-TAATACGACTCACTATA-3') and PPT-E5rev (5'-GTGAGAGATCTGACCATGCC-3') with 18 cycles was performed using annealing and extension temperatures of 70 and 72 °C, respectively. PCR products were resolved on a 5% nondenaturing polyacrylamide gel. Bands were quantified directly from the gel using a phosphor imager. The percentage of inclusion is the percentage of

<sup>2</sup> This calculation can be performed on the World Wide Web at <http://cookie.imcb.osaka-u.ac.jp/stamm/>.

<sup>3</sup> The servers can be found on the World Wide Web at <http://www-genome.wi.mit.edu/cgi-bin/contig/rhmapper.pl> and <http://www.ncbi.nlm.nih.gov/cgi-bin/SCIENCE96/msrch2?CHR=16>.

spliced RNA that contains the exon (cpm of inclusion band/(cpm of inclusion band + cpm of exclusion band)  $\times$  100.

### RESULTS

**Sequence**—In order to find new proteins involved in RNA processing, we performed yeast two-hybrid screens with SRp30c (4) and identified a clone from a HeLa library, which we named Nop30. Its sequence is shown in Fig. 1A. The cDNA of Nop30 encodes a protein with a calculated molecular mass of 24.3 kDa. The protein contains a highly acidic N terminus (amino acids 1–95) with an isoelectric point of 4.9 and a basic C terminus, enriched with arginines, serines, and prolines (amino acids 96–124) ( $pI = 12.7$ ). The total protein is highly basic ( $pI = 11.7$ ) (Fig. 1B). Probably due to the bipolar charge distribution, it has an apparent molecular mass of 30 kDa upon SDS gel electrophoresis. Inspection of the sequence shows that it contains a potential cAMP-dependent protein kinase phosphorylation site (amino acids 197–200), several potential protein kinase C phosphorylation sites, and a potential casein kinase II phosphorylation site (amino acids 41–44). The casein kinase II site may be functional, since recombinant protein can be phosphorylated by casein kinase II *in vitro* (data not shown). Due to the presence of arginine and serine residues (Fig. 1D), the C terminus of Nop30 shows homology to some SR and SR-related proteins (human protein kinase CLK3 (23) and splicing factors 9G8, SRp55, SRp75, and SC35 (2)).

Data base searches also showed that the first 95 amino acids of Nop30 share 94% homology to a rat protein with an as yet unknown function that was previously found in a screen aimed to identify genes induced with nerve growth factor (13). However, due to a frameshift, the carboxyl domains encoded by the two cDNAs are completely different. We searched the expressed sequence tag data base (25) and identified a human clone (accession number AA085275) corresponding to the rat cDNA. This expressed sequence tag clone was entirely sequenced and found to encode the human homologue of the rat cDNA clone described by Geertman *et al.* (13). The carboxyl terminus of the encoded protein is characterized by clusters of prolines and glutamic acids (Fig. 1, A and B). We named this protein Myp (muscle-enriched cytosolic protein) because of its expression pattern and intracellular localization (see below). In addition to the different C terminus caused by the frameshift, this clone differs from our two-hybrid isolate by the use of a different polyadenylation site (PS-2, Fig. 1A).

Since both human sequences differ by only ten nucleotides in their coding region, they could derive from alternative splicing. We therefore screened a human BAC library and obtained a genomic *NOP* clone. Comparison of its sequence with Nop30 and its variant revealed that the gene is composed of four exons and three introns and generates the two isoforms by using an alternative 5' splice site in exon 2 (Fig. 1, A and C). The size of the gene is at least 1800 nucleotides. The same first start codon present in all expressed sequence tags, our two-hybrid isolate, and the rat cDNA is located in exon II. In contrast to rat, the start codon in humans deviates slightly from the Kozak consensus sequence (26). A remarkable feature of the gene is the small size of its introns (115 nucleotides for intron A, 155/165 nucleotides for intron B, and 102 nucleotides for intron C). This is significantly smaller than mammalian internal introns, which average around 1127 nucleotides (27). All intron/exon boundaries are in agreement with the mammalian consensus sequence. However, calculation of the splice site scores revealed a difference in the alternatively used 5' splice site of intron B. The splice site generating Nop30 (score 5.3) deviates from the average score of constitutive exons (score 8.1), which is typical for a subset of alternatively spliced exons (18). In contrast, the score of the variant splice site (score 7.9) is close

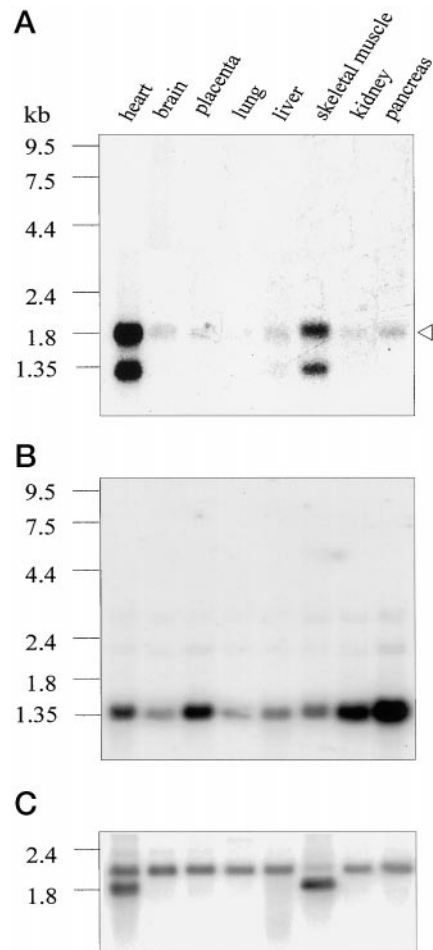


**FIG. 3. Northern blot analysis of Nop30 expression.** A, Northern blot analysis of *NOP* transcripts on various human tissues (CLONTECH) using a full-length Nop30 probe. The signals at 1.8 and 1.3 kb in heart and skeletal muscle correspond to *NOP* transcripts processed at the two polyadenylation sites. The faint band detected in nonmuscle tissues is indicated by a triangle. B, the same filter was rehybridized with a human SRp30c full-length probe. The highest expression was detected in pancreas, followed by kidney, placenta, and heart. C, the same filter was rehybridized with a  $\beta$ -actin control probe. The cytoskeletal  $\beta$ -actin isoform is detected at 2.0 kb. The probe also hybridizes to the muscle-specific  $\alpha$  and  $\gamma$  isoforms (1.8 kb) in heart and muscle.

to the average score of constitutive exons (score 8.1).

Using the Stanford radiation hybrid panel with the primers PEint1 and PEintof1, we mapped the *NOP* gene to human chromosome 16. The *NOP* gene was found 3.15 cR from WI-5594, between markers WI-5594 and WI-9392 (Fig. 2). This most likely corresponds to the region between 81 and 84 cM on chromosome 16 (q21 to q23). In summary, we have shown that the *NOP* gene is located on chromosome 16q and generates two isoforms via an alternative splicing mechanism.

**Expression**—We next determined the expression of *NOP* and performed Northern blot analysis with various human tissues using the full-length cDNA fragment of Nop30 as a probe. Nop30 mRNA shows the highest expression in heart and skeletal muscle (Fig. 3A). However, a faint band is visible in other tissues examined. The two bands of 1.8 and 1.3 kb most likely correspond to the two polyadenylation sites found in the *NOP* gene (Fig. 1A). These expression data are in agreement with the tissue distribution found for the rat cDNA (13). The 1.8-kb band corresponds to the size of the longest cDNA clone, indicating that we have obtained the full-length Nop30 transcripts. By probing mouse tissue with a human cDNA probe, it was shown that SRp30c is predominantly expressed in kidney,

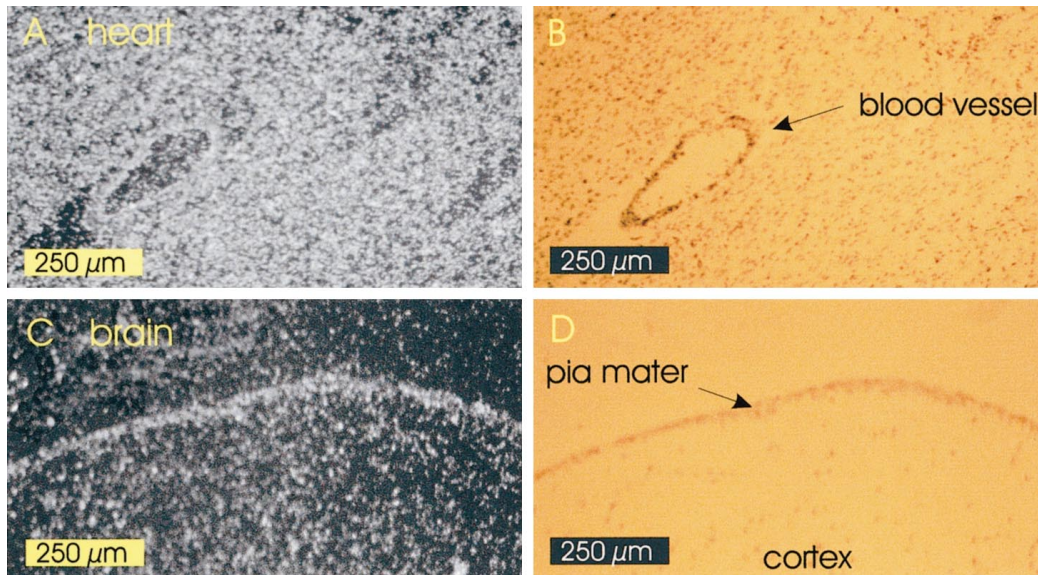


FIG. 4. *In situ* analysis of Nop30 expression in heart and brain. *A*, dark field picture of rat heart tissue probed with a rat Nop30 antisense cRNA. *B*, cresyl violet counterstain of the same area as in *A*. The blood vessel present in this area is indicated. *C*, dark field picture of rat brain probed with Nop30 antisense cRNA. The signal is located in the pia mater. No tissue is present between the top of this section and the pia mater. The signal there represents the background. *D*, cresyl violet counterstain of the same area as in *C*.

lung, and spleen, whereas only low levels were detected in muscle (4). This expression pattern would make an *in vivo* interaction between SRp30c and Nop30 questionable. We therefore reprobbed our filter with human SRp30c and found considerable SRp30c expression in human striated muscle as well as in other tissues (Fig. 3*B*), suggesting that SRp30c is a possible interactor for Nop30 in muscle. The same blot was reprobbed with a  $\beta$ -actin control (CLONTECH) to verify that equivalent amounts of RNA were loaded. In heart and skeletal muscle, the additional muscle-specific actin isoforms at 1.8 kb were detected (28).

We noticed a faint signal present in nonmuscle tissues using Nop30 as a probe (Fig. 3*A*) and compared Nop30 mRNA expression in heart and brain using *in situ* hybridization. We used a rat Nop30 cDNA fragment containing the whole coding region, except for the C-terminal repetitive sequence, as a probe. The Nop30 antisense probe gave a strong signal after *in situ* hybridization in heart (Fig. 4*A*). In brain, a specific signal was only seen in the pia mater (Fig. 4*C*). The pia mater is of mesenchymal origin, surrounds the brain (Fig. 4*D*), and contains blood vessels lined with smooth muscle cells (29). In contrast, the signal derived from neuronal or glial cells did not exceed the background. No signal could be detected using a sense control probe (data not shown). In summary, Northern blot analysis and *in situ* hybridization demonstrate that Nop30 shows the highest expression in muscle cells. Moreover, using RT-PCR, we did not detect a change in expression during C2C12 cell differentiation into myoblasts or during embryonic development, suggesting that Nop30 mRNA and its isoform are constitutive parts of muscle cells in various stages of differentiation and development (data not shown).

**Interaction with Other Proteins**—In order to obtain information on the possible function of Nop30 and its isoform, we tested its interaction with other proteins in the yeast two-hybrid system. Of all proteins involved in pre-mRNA metabolism tested (SRp20, SF2/ASF, SC35 (2), SmN (30), htra-beta1 (21), SRp30c, SRp75, SRp55, (4) SAF-B (5), U2AF35 (31), and the carboxyl-terminal domain of RNA polymerase II (8)), only SRp30c and Nop30 itself showed interaction in yeast (Fig. 5*A*). Interestingly, its splice variant Myp did not interact with SRp30c and reacted only weakly with Nop30. This indicated

that the different carboxyl termini of the two splice variants are responsible for differences in protein-protein interactions. We therefore tested them separately. The deletion constructs used are shown schematically in Fig. 5*B*. We found that deletion of the N terminus of Nop30 abolishes binding to Nop30, whereas a clone with a deleted C terminus was still able to interact. In addition, the two C-terminal Nop30 deletion variants (Nop30 $\Delta$ C) were also found to interact. Thus, Nop30 dimerizes or multimerizes via its N terminus. In contrast, deleting either the C or N-terminal part of Nop30 resulted in a lack of interaction with SRp30c. In addition, deletion of the RS domain of SRp30c prevented binding of SRp30c to Nop30 (Fig. 5*A*). We conclude from this analysis that Nop30 interacts with the RS domain of SRp30c, using parts of both its N- and C-terminal domain.

In order to verify the two-hybrid interactions biochemically, Nop30 was translated and incubated *in vitro* with glutathione-Sepharose, GST, GST-SRp30c, and GST-ASF/SF2 (Fig. 6). In this assay, Nop30 bound only to SRp30c, but not to SF2/ASF. This confirmed our two-hybrid analysis and indicated that Nop30 can discriminate between the related RS domains of SF2/ASF and SRp30c.

Next, we tested Nop30 interaction under more physiological conditions in immunoprecipitation assays. We fused Nop30, Myp, SRp30c, and their deletion variants previously analyzed in yeast (Fig. 5*B*) to EGFP and co-transfected these constructs with FLAG-tagged Nop30, SRp30c, and ASF/SF2 in HEK293 cells. Complexes were precipitated with a monoclonal anti-EGFP antibody, and interacting proteins were detected with an anti-FLAG antibody. As shown in Fig. 7*A*, Nop30 bound to itself, more weakly to its amino terminus (Nop30 $\Delta$ C), and to SRp30c. As in yeast, there was no detectable interaction between EGFP-Nop30 and FLAG-SF2/ASF. The variant EGFP-Myp did not bind to FLAG-SRp30c, and EGFP alone did not interact with FLAG-Nop30 and FLAG-SRp30c (Fig. 7*A*, lanes 9 and 10). Despite inclusion of protease inhibitors, a nonspecific background was repeatedly observed in our experiments (Fig. 7*A*, lanes 3, 5, 6, and 7), which might be due to proteolytic fragmentation of the antibody used in the immunoprecipitation. Fig. 7*B* demonstrates that all EGFP-tagged constructs were immunoprecipitated with the anti-GFP antibody and mi-



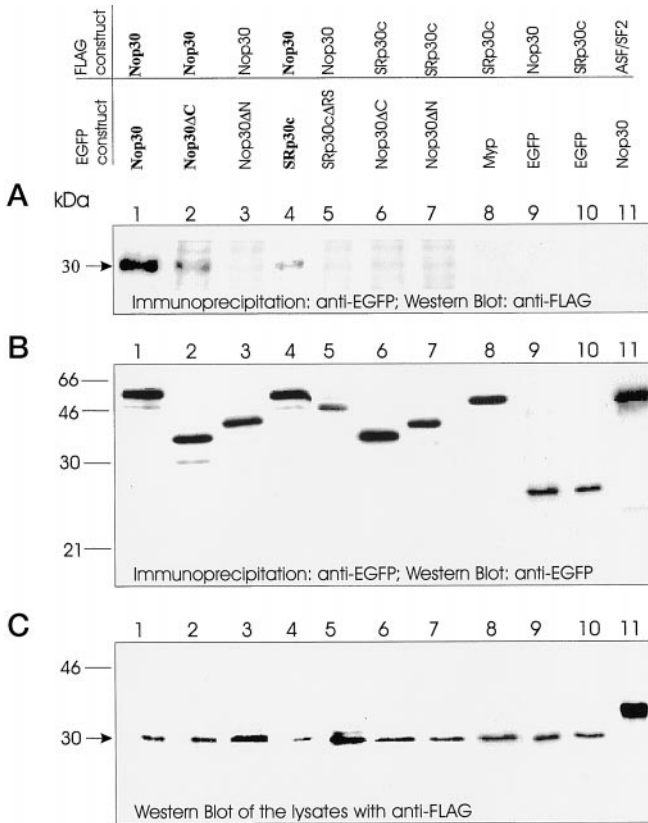


**FIG. 7. Detection of Nop30 interactions by immunoprecipitation.** 0.1  $\mu$ g of plasmid DNA encoding the EGFP and FLAG fusion proteins indicated in A (top) was transfected into HEK293 cells. A, The EGFP constructs were immunoprecipitated with a monoclonal anti-GFP antibody, and the co-immunoprecipitating FLAG-constructs were detected with an anti-FLAG antibody. Immunoprecipitated binding partners are indicated in *boldface type*. The location of FLAG-Nop30 that migrates at 30 kDa is indicated by an arrow on the left. B, Western blot with anti-GFP antibody to detect the precipitated EGFP fusion protein. The fusion proteins migrate according to their molecular masses indicated: EGFP-Nop30, 51 kDa; EGFP-Nop30 $\Delta$ N, 38 kDa; EGFP-Nop30 $\Delta$ C, 41 kDa; EGFP-Myp, 50 kDa; EGFP-SRp30c, 52 kDa; EGFP-SRp30c $\Delta$ SR, 48 kDa; EGFP, 27 kDa. C, Western blot with an anti-FLAG antibody of the cell lysates prior to immunoprecipitation. FLAG-SRp30c and FLAG-Nop30 fusion proteins migrate at 30 kDa; FLAG ASF/SF2 (lane 11) migrates slightly more slowly.

(32–34). We therefore performed localization experiments with the nucleolar protein B23, which is a marker for the granular component of nucleoli (34). As shown in Fig. 9, D–F, Nop30 and B23 colocalize in the granular component of nucleoli. It is also evident that the major part of Nop30 localizes in the area between the foci and the granular component, which is likely to be the fibrillar component according to the classical organization of the nucleolus (35).

To determine whether an interaction between Nop30 and SRp30c can take place *in vivo*, we analyzed the localization of EGFP-Nop30 and FLAG-SRp30c (Fig. 9, G–I) using an anti-FLAG antibody. SRp30c does not localize in nucleoli, but both proteins were detected in the nucleoplasm, indicating that the interaction between both proteins could occur *in vivo*.

We next tested Myp, the splice variant of Nop30. Transfection of the EGFP-tagged variant revealed that it is predominantly located in the cytoplasm. Only faint staining could be detected in the nucleus, and no staining was detected in nucleoli (Fig. 10A). Therefore, we named this protein Myp (muscle-enriched cytoplasmic protein). Since the intracellular localization of Myp and Nop30 is different, we tested their common N terminus and different C termini separately. The common N

terminus gave a predominant cytoplasmic staining pattern resembling Myp (Fig. 10C). Transfection of cells with the C terminus of Nop30 resulted in nuclear staining, with predominant staining in the nucleoli similar to that of full-length Nop30 (Fig. 10D). In contrast, when we tested the C terminus of Myp, we observed staining throughout the cell, excluding the nucleoli (Fig. 10B). The integrity of various EGFP constructs used for fluorescence was tested by Western blot (Fig. 10E), demonstrating that all constructs expressed protein of the expected size.

We conclude from these experiments that the two splice variants generated by the *NOP* gene have a different intracellular localization; Nop30 is a nuclear protein concentrated in the nucleoli, and the variant Myp is predominantly localized in the cytoplasm. The localization to nucleoli is an intrinsic property of the basic arginine-rich C terminus of Nop30, whereas the acidic N terminus seems to exclude the protein from the nucleus.

*In Vivo Splicing*—We next asked whether the binding properties of Nop30 to SRp30c are relevant *in vivo*. Since concentration changes of SR proteins modulate alternative splicing patterns *in vivo* (3, 36, 37), we reasoned that overexpression of Nop30 would change the SR protein composition through interaction with SRp30c, which would change splicing patterns of a reporter gene. First, we employed the SRp20 XB minigene. Using this construct, it has been shown that SRp20 can promote inclusion of the alternative exon 4 in its own mRNA, whereas SF2/ASF has the opposite effect (14). We examined the effect of Nop30 on exon 4 usage (Fig. 11A) and cotransfected the SRp20 XB minigene with an increasing ratio of pNop30-C2 to the parental vector pEGFP-C2 (Fig. 11, A–C, top). With increasing amounts of pNop30-C2, we detected a decrease of exon 4 inclusion from ~34 to 10% (Fig. 11A). In order to compare the effect of SRp30c on this minigene, we performed a similar experiment and found that EGFP-SRp30c also decreases exon 4 usage (Fig. 11B). However, less EGFP-SRp30c cDNA needs to be transfected to reduce exon 4 usage. To examine the combined effect of SRp30c and Nop30 on exon 4 splicing, we performed cotransfection experiments in which increasing amounts of pNop30c were added to a constant amount of SRp20 XB minigene and SRp30c (Fig. 11C). We found that, in the presence of EGFP-SRp30c, less pNop30-C2 was necessary to induce a visible decrease in exon 4 usage. Transfection of 5  $\mu$ g of pNop30-C2 abolished inclusion of the alternative exon (Fig. 11C), whereas this amount of pNop30-C2 did not change exon 4 usage significantly in the absence of SRp30c (Fig. 11A). Overexpression of EGFP alone (first lane in each experiment) did not induce exon skipping. To test the effect of Nop30 in another system, we used a PPT minigene (38). As shown in Fig. 11D, cotransfection of 3 and 10  $\mu$ g of pNop30-C2 promotes alternative exon inclusion in the PPT system, again indicating that concentration changes of Nop30 changes alternative exon usage *in vivo*. In contrast, overexpression of the splicing factor SC35 had no significant effect on exon 4 inclusion. We conclude from these experiments that Nop30 can influence alternative splicing *in vivo*.

#### DISCUSSION

We report on the molecular cloning and characterization of the *NOP* gene and its two products, which are generated by alternative splicing. Northern blot analysis indicates that the gene is predominantly expressed in muscle cells. In order to investigate a weak signal present in all tissues examined, we performed *in situ* hybridization with rat brain sections and found that the *NOP* gene is expressed in the pia mater, indicating a specific expression pattern. Therefore, we assume that the faint signal detected in nonmuscle tissues with Northern

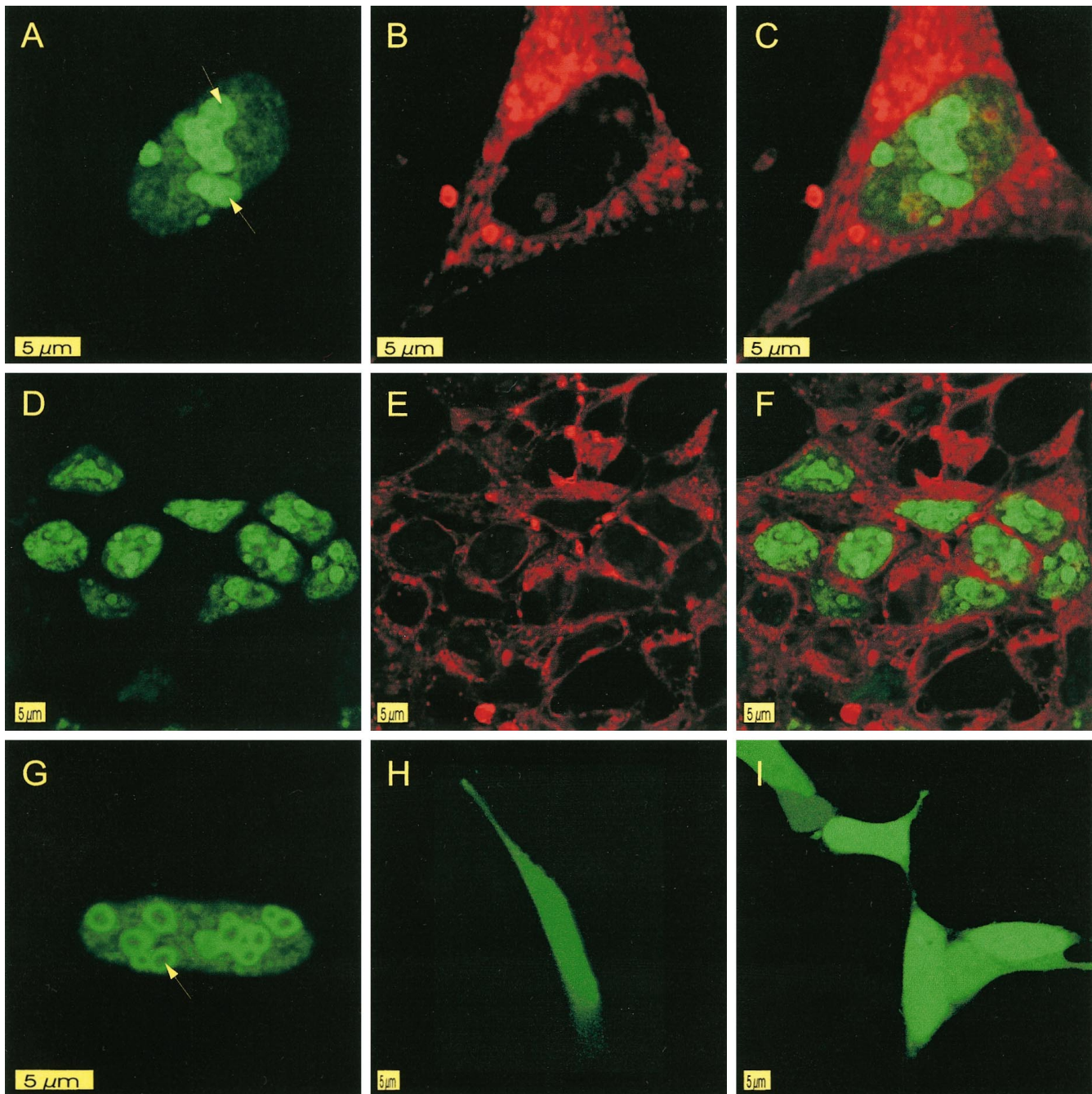


**FIG. 8. Intracellular localization of Nop30.** *A*, pNop30-C2 expressing EGFP-Nop30 was transfected in BHK cells. The protein is present in the nucleoplasm and is enriched in nucleoli excluding discrete foci (arrows). *B*, the same cell stained with DiI. *C*, overlay of *A* and *B*. *D*, expression of EGFP-Nop30 in HEK293 cells. The pattern is similar to that of BHK cells. *E*, the cells of *D* were counterstained with DiI. *F*, overlay of *D* and *E*. *G*, BHK cell transfected with pNop30-C2. Instead of multiple foci as in *A*, some cells have a large region inside the nucleoli from which Nop30 is absent. *H*, BHK cell expressing EGFP. *I*, HEK293 cells expressing EGFP.

blot analysis might result from muscle-derived cells that line blood vessels in all tissues. Therefore, it is possible that Nop30 expression is muscle-specific. However, from our data we cannot exclude a weak basal *NOP* expression in other tissues. The *NOP* gene is located on chromosome 16 between 16q21 and 16q23. Although only a few genes are identified in this region, it is interesting that a 16q23.1 deletion leads to disorders in musculoskeletal systems (39). Further analysis will be necessary to investigate whether Nop30 is involved in one of these disorders.

The Nop30 cDNA was obtained in a two-hybrid screen for proteins that interact with SRp30c. Using the three independent methods of yeast two-hybrid assays, GST pull down exper-

iments and immunoprecipitations, we were able to demonstrate that Nop30 protein can bind to itself and to SRp30c. The multimerization of Nop30 protein depends on its N terminus. The interaction with SRp30c is dependent on the RS domain of SRp30c and both N- and C-terminal parts of Nop30. Our results demonstrate that protein-protein interactions mediated by RS domains can be extremely specific. In order to test whether an interaction of Nop30 with SRp30c is possible *in vivo*, we determined the distribution of SRp30c in human tissues. We found that human SRp30c is found in all tissues, including muscle. Furthermore, we show that both SRp30c and Nop30 colocalized in the nucleoplasm (Fig. 9, *G-I*). Taking the expression and localization experiments together, it is likely

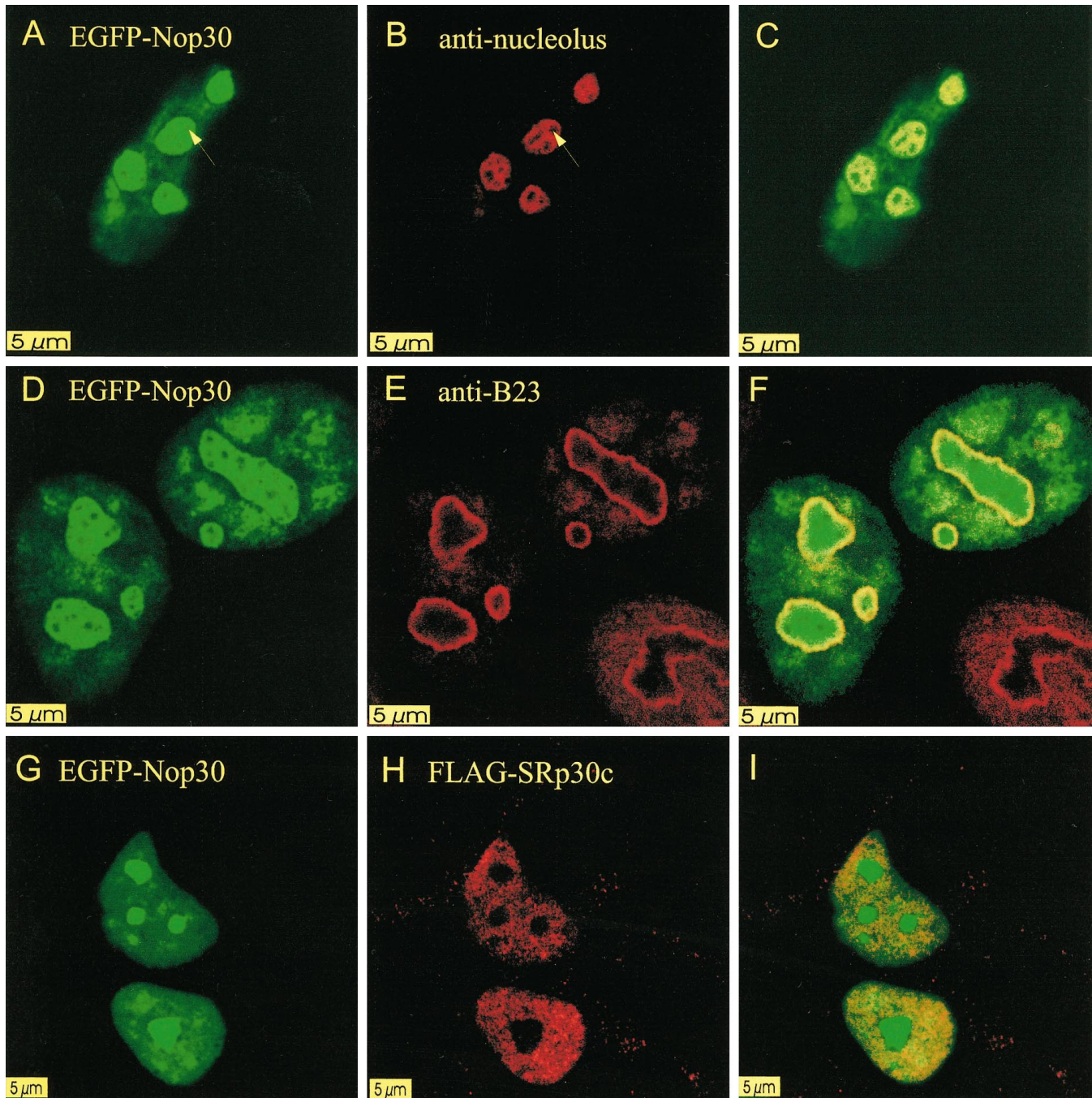


**FIG. 9. Colocalization experiments with nucleolar antigens or SRp30c.** *A*, HEK293 cells expressing EGFP-Nop30. The unstained foci are indicated by an arrow. *B*, the same cell was stained with an anti-nucleolus antibody (Calbiochem). *C*, overlay of *A* and *B*. Colocalization is indicated by yellow color. *D*, HEK293 cells transfected with pNop30-C2. *E*, the same cells as in *D* were stained with a monoclonal anti-B23 antibody (22), which marks the granular component of the nucleoli. *F*, colocalization of EGFP-Nop30 and B23 is indicated by yellow color. *G*, HEK293 cells expressing EGFP-Nop30. *H*, the same cells as in *G* expressing FLAG-SRp30c. *I*, colocalization of EGFP-Nop30 and FLAG-SRp30c is observed in the nucleoplasm but not in the nucleoli.

that Nop30 interacts with SRp30c in the nucleoplasm of muscle cells.

Alternative splicing is a commonly used mechanism to create protein isoforms (1, 40). A usual feature of alternatively used exons is the introduction of stop codons or frameshifts (18) that can either switch off genes (41) or create proteins with different C termini, which can result in a different intracellular localization. For example, the nuclear localization of the estrogen receptor (42) and the transcription factors E2F (43), p105 NF- $\kappa$ B (44), and a protein-tyrosine phosphatase (45) as well as the intracellular localization of the NADH-cytochrome  $b_5$  reductase (46) are controlled by alternative splicing. In the *NOP*

gene, the intracellular localization of the gene products is dependent on alternative 5' splice site usage, causing a frameshift that creates two different carboxyl termini. Nop30 is found in the nucleoplasm and is concentrated in the nucleoli, whereas its variant Myp is distributed throughout the cytosol. Myp did not interact with SRp30c (Fig. 5A), indicating that alternative splicing determines the binding specificity of the *NOP* gene products. Therefore, in muscle, the amount of the interactor of the splicing factor SRp30c could be regulated by alternative splicing. This is reminiscent of other proteins involved in pre-mRNA splicing that are regulated by alternative splicing. For example, in mammals, splice variants of SRp55,

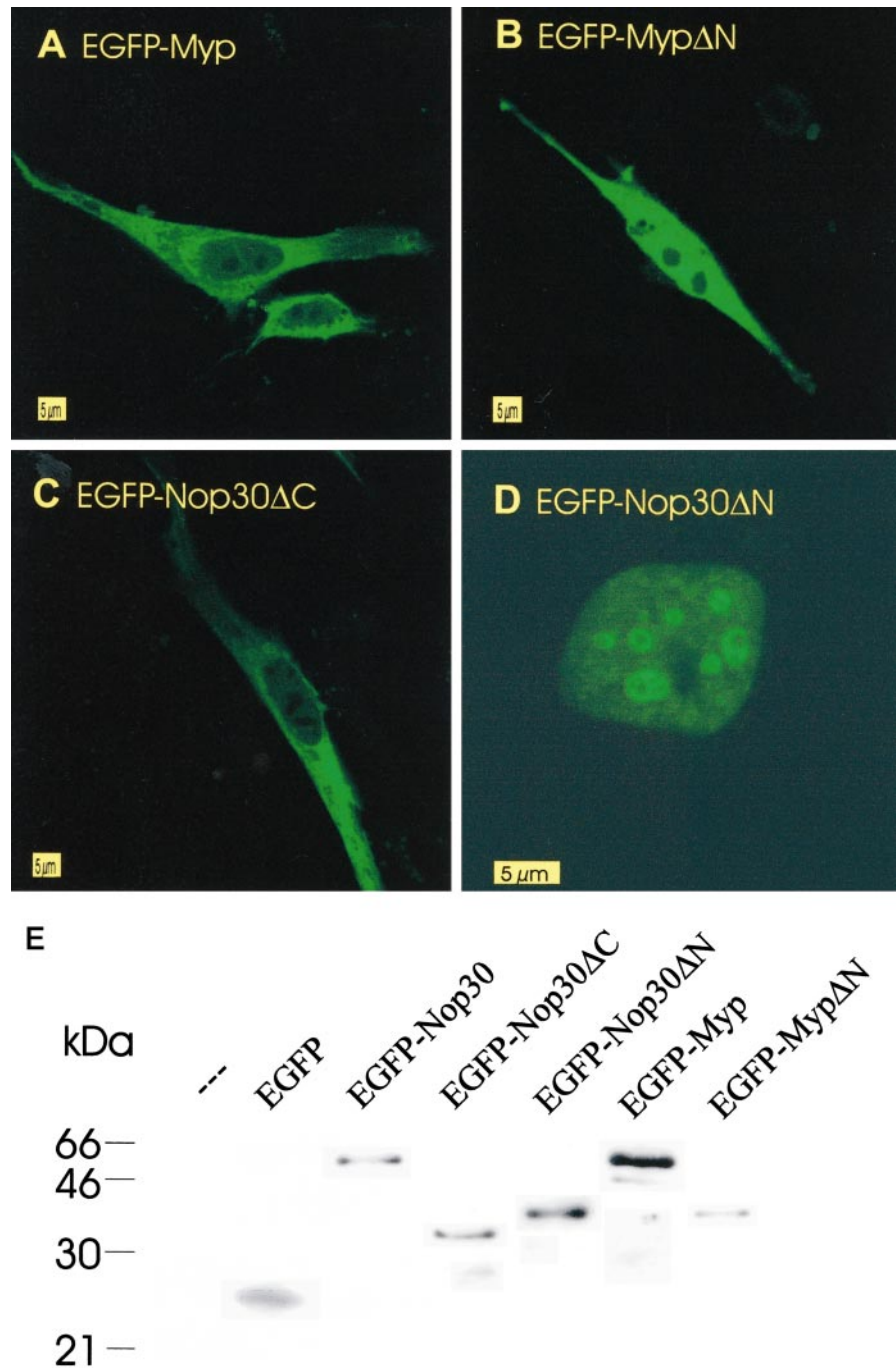


**FIG. 10. Intracellular localization of Myp and Nop30 deletion variants.** BHK cells were transfected with the EGFP-tagged constructs indicated. *A*, EGFP-Myp localizes predominantly in the cytoplasm with a weak nuclear staining. *B*, the C terminus of Myp (EGFP-Myp $\Delta$ N; amino acids 99–208) is distributed throughout the whole cell excluding the nucleoli. *C*, N terminus of EGFP-Nop30 (EGFP-Nop30 $\Delta$ C; amino acids 1–95). The localization is primarily cytoplasmic. *D*, the C terminus of EGFP-Nop30 (EGFP-Nop30 $\Delta$ N; amino acids 96–219) localizes, similar to full-length Nop30, in nucleoli and is also present in the nucleoplasm without a cytoplasmic staining. *E*, Western blot of EGFP constructs used in the transient transfection assays. Immunoprecipitation was performed with a monoclonal anti-GFP antibody (Boehringer Mannheim); detection was performed with a polyclonal rabbit anti-GFP antibody (CLONTECH). The fusion proteins have the following molecular masses: EGFP, 27 kDa; EGFP-Nop30, 51 kDa; EGFP-Nop30 $\Delta$ C, 41 kDa; EGFP-Nop30 $\Delta$ N, 38 kDa; EGFP-Myp, 50 kDa; EGFP-Myp $\Delta$ N, 39 kDa.

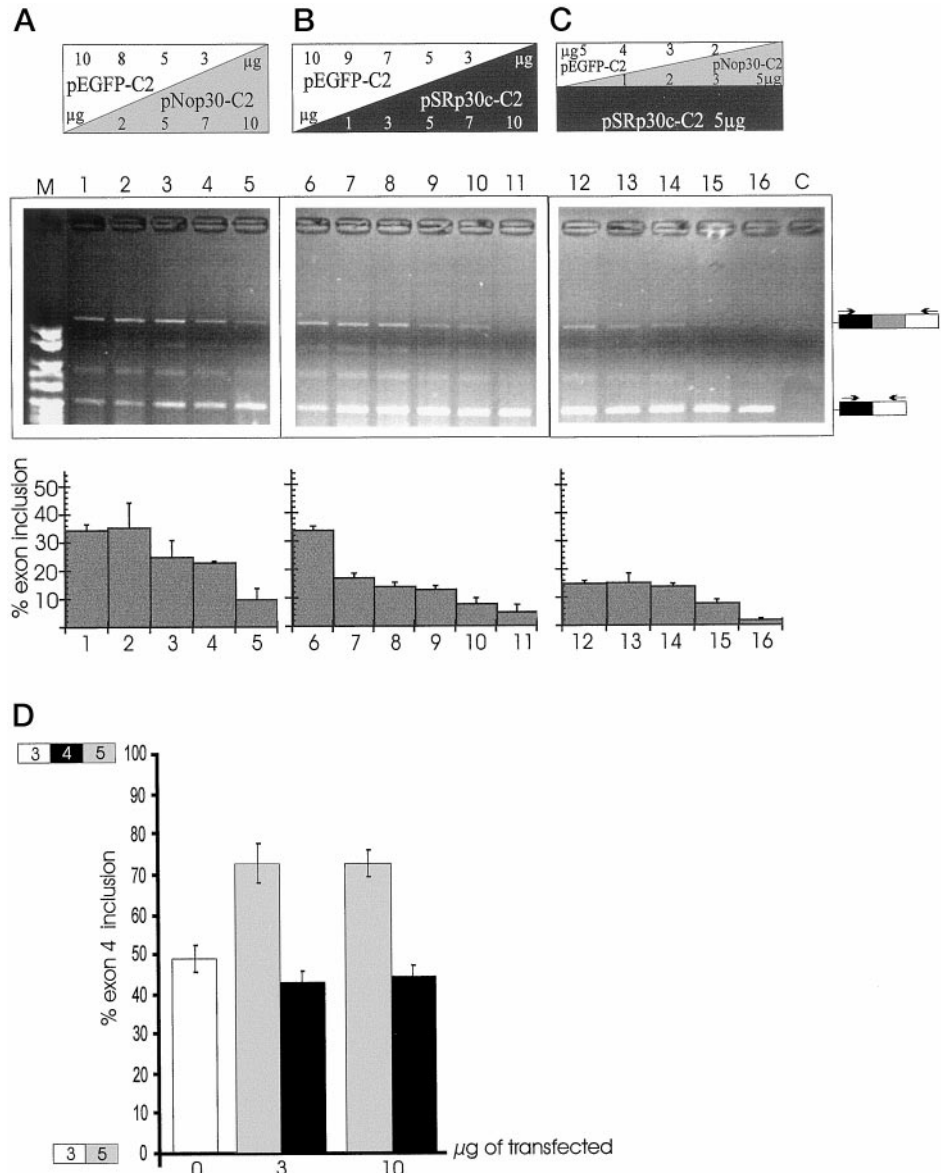
SRp40 (4, 47), and ASF/SF-2 (48), and the mammalian homologue of SWAP (49) and transformer-2 (21) have been described. In the case of transformer-2 (50), SWAP (51), and X16/SRp20 (14), the alternative splicing event seems to be autoregulated.

Nucleoli vary in size and shape, reflecting the cellular activity (52, 53). In addition, nucleoli of transformed cells have been reported to be extremely irregular in number, shape, and size (54, 55), as can also be seen in our Figs. 8 and 9. No significant difference between nucleoli of transfected and untransfected cells was observed by bright field and fluorescence microscopy using the B23 antibody (Fig. 9F), indicating that Nop30 overexpression does not change the nucleolar shape. Nop30 protein expression is restricted to specified areas in the nucleolus. Colocalization with B23 revealed that Nop30 is present in the granular component, where the later stages of ribosome bio-

synthesis occur. In addition, it is detected in the more central region that could be the dense fibrillar component. Furthermore, we noticed that, based on their size, number, and shape (56, 57), Nop30 is absent from discrete foci that are most likely the fibrillar centers.

The function of Nop30 proteins has yet to be demonstrated directly. Colocalization and binding to SRp30c suggest a role of Nop30 in pre-mRNA processing. Indeed, we found an effect of Nop30 on splicing of a PPT and a SRp20 reporter gene *in vivo*. As with all mammalian factors involved in pre-mRNA processing, the specific target gene is unknown (3). Nop30 has a different effect on the two minigenes tested; it promotes exon inclusion in the PPT minigene but causes exon skipping when tested with the SRp20 construct. This is reminiscent of opposing effects of splicing factors on natural minigenes *in vivo*. For example, SF2/ASF promotes exon EN inclusion when tested

**FIG. 11. *In vivo* splicing assays.** A, a total amount of 10  $\mu\text{g}$  of an increasing ratio of pNop30-C2 (encoding EGFP-Nop30) to empty vector pEGFP-C2 was cotransfected with 2  $\mu\text{g}$  of the SRp20 XB minigene in HEK293 cells and analyzed by RT-PCR. The amount of transfected EGFP constructs is indicated at the top of the gel. PCR products were stained with ethidium bromide and quantified. The size difference between the upper and the lower band corresponds to the size of alternative exon 4 (435 nucleotides). The structure of the PCR products is indicated schematically on the right. Primers used are indicated as arrows. Exon 4 inclusion was calculated as follows: (amount of inclusion band/(amount of inclusion band + amount of exclusion band))  $\times$  100. The percentage of exon inclusion is shown under each gel. Error bars represent the S.D. from three independent experiments. M, pBR322 *Msp*I digest. B, a similar experiment as in A was performed with pSRp30c-C2 instead of pNop30-C2. C, *in vivo* splicing was investigated using a total amount of 10  $\mu\text{g}$  of a mixture of three different EGFP constructs (pNop30-C2, pSRp30c-C2, and pEGFP-C2) and 2  $\mu\text{g}$  of the SRp20 minigene. The amount of transfected pSRp30c-C2 was 5  $\mu\text{g}$  in every case, whereas 5  $\mu\text{g}$  of an increasing ratio of pNop30-C2 (encoding EGFP-Nop30) to empty vector (pEGFP-C2) were cotransfected. D, chicken fibroblast cells were cotransfected with 2  $\mu\text{g}$  of PPT minigene and 0, 3, and 10  $\mu\text{g}$  of either pNop30-C2 or pCG35 (expressing SC35). Control, only the PPT minigene was transfected. RNA was isolated, and splicing of the minigene was analyzed by radioactive RT-PCR with the primer pair T7PRO and PPT5rev. The RT-PCR products containing exon 4 were separated from those lacking exon 4 on a 5% polyacrylamide gel. The quantification of three independent experiments is shown. Exon inclusion was calculated as follows: (cpm of inclusion band/(cpm of inclusion band + cpm of exclusion band))  $\times$  100. White bar, control; shaded bars, pNop30-C2; black bars, pCG35.



with the clathrin light chain B minigene (36) but causes exon 4 skipping with the SRp20 minigene (14).

The predominant nucleolar localization of Nop30 also points to a potential role in RNA processing in muscle nucleoli. There are several examples of intimate connections between nuclear compartments. For example, in *S. cerevisiae* rRNA processing and pre-mRNA splicing are coupled via the ribosomal protein L32, which influences both splicing of its own transcript and the processing of rRNA (58). Another link between splicing and nucleolus comes from the observation that the transcript of the mouse ribosomal protein S24 gene is alternatively spliced (59). Therefore, it seems likely that Nop30 has a dual role in splicing as well as in the nucleolus.

Several studies *in vivo* (3, 36, 37, 60) and *in vitro* (3, 4, 48, 61, 62) have shown that SR protein concentration can influence alternative splice site selection. Specifically, an increase in the nuclear concentration of a transiently overexpressed SR protein changes alternative exon usage. Tissue-specific differences in the ratio of SR proteins and hnRNP A1 suggest a role in tissue-specific splicing (63), and alterations in the levels of individual SR proteins have been associated with changes in CD44 alternative splicing during T cell activation (4). Therefore, SR proteins are likely to be involved in tissue-specific

regulation of alternative splicing. Due to its binding properties to SRp30c, its ability to influence splice site decisions, and its high expression in muscle, it is possible that Nop30 changes the free concentration of SRp30c by specifically sequestering this SR protein in muscle cells. This muscle-specific sequestration would change the SR protein composition in a cell type-specific way and might indirectly lead to muscle-specific alternative splicing decisions. Alternatively, similar to results obtained with SRm160 (64), it is possible that Nop30 enhances effects of SR proteins on certain genes, which would be consistent with the synergistic effect of Nop30 and SRp30c on exon 4 of the SRp20 minigene (Fig. 11C). It remains to be seen whether other tissue-specific proteins exist that can discriminate between different SR proteins and might influence alternative splicing.

**Acknowledgments**—We thank Clair Lo for excellent technical assistance, Claudia Cap for sequencing, and Peter Nielsen for providing the SRp20 minigenes. We thank Robert Ochs for sending us the B23 antibody and Petra Kioschis from the German Genome Center for performing the genomic screen.

## REFERENCES

- Krämer, A. (1996) *Annu. Rev. Biochem.* **65**, 367–409
- Fu, X.-D. (1995) *RNA* **1**, 663–680
- Manley, J. L., and Tacke, R. (1996) *Genes Dev.* **10**, 1569–1579

4. Sreaton, G. R., Caceres, J. F., Mayeda, A., Bell, M. V., Plebanski, M., Jackson, D. G., Bell, J. I., and Krainer, A. R. (1995) *EMBO J.* **14**, 4336–4349
5. Nayler, O., Strätling, W., Bourquin, J.-P., Stagljar, I., Lindemann, L., Jasper, H., Hartmann, A. M., Fackelmeyer, F. O., Ullrich, A., and Stamm, S. (1998) *Nucleic Acids Res.* **26**, 3542–3549
6. McCracken, S., Fong, N., Yankulov, K., Ballantyne, S., Pan, G., Greenblatt, J., Patterson, S. D., Wickens, M., and Bentley, D. L. (1997) *Nature* **385**, 357–361
7. Corden, J. L., and Patturajan, M. (1997) *Trends Biochem. Sci.* **22**, 413–416
8. Bourquin, J.-P., Stagljar, I., Meier, P., Moosmann, P., Silke, J., Baechli, T., Georgiev, O., and Schaffner, W. (1997) *Nucleic Acids Res.* **25**, 2055–2061
9. Steinmetz, E. J. (1997) *Cell* **89**, 491–494
10. Melese, T., and Xue, Z. (1995) *Curr. Opin. Cell Biol.* **7**, 319–324
11. Shaw, P. J., and Jordan, E. G. (1995) *Annu. Rev. Cell. Dev. Biol.* **11**, 93–121
12. Schul, W., de Jong, L., and van Driel, R. (1998) *J. Cell. Biochem.* **70**, 159–171
13. Geertman, R., McMahon, A., and Sabban, E. L. (1996) *Biochim. Biophys. Acta* **1306**, 147–152
14. Jumaa, H., and Nielsen, P. J. (1997) *EMBO J.* **16**, 5077–5085
15. Fields, S., and Song, O. (1989) *Nature* **340**, 245–247
16. Genetics Computer Group (1994) *Program Manual for the Wisconsin Package*, Version 8, Genetics Computer Group, Madison, WI
17. Sambrook, J., Fritsch, E. F., and Maniatis, T. (1989) *Molecular Cloning: A Laboratory Manual*, Cold Spring Harbor Laboratory, Cold Spring Harbor, NY
18. Stamm, S., Zhang, M. Q., Marr, T. G., and Helfman, D. M. (1994) *Nucleic Acids Res.* **22**, 1515–1526
19. Schmitt, A. B., Gotzes, S., Voel, M., Schwaiger, F.-W., Spitzer, C., Pech, K., Brook, G. A., Noth, J., and Nacimiento, W. (1999) *J. Neurobiol.*, in press
20. Chen, C., and Okayama, H. (1987) *Mol. Cell. Biol.* **7**, 2745–2752
21. Beil, B., Sreaton, G., and Stamm, S. (1997) *DNA Cell Biol.* **16**, 679–690
22. Ochs, R., Lischwe, M., O'Leary, P., and Busch, H. (1983) *Exp. Cell Res.* **146**, 139–149
23. Nayler, O., Stamm, S., and Ullrich, A. (1997) *Biochem. J.* **326**, 693–700
24. Laemmli, U. K. (1970) *Nature* **227**, 680–685
25. Lennon, G. G., Auffray, C., Polymeropoulos, M., and Soares, M. B. (1996) *Genomics* **33**, 151–152
26. Kozak, M. (1984) *Nucleic Acids Res.* **12**, 857–872
27. Hawkins, J. D. (1988) *Nucleic Acids Res.* **16**, 9893–9908
28. Pari, G., Jardine, K., and McBurney, M. W. (1991) *Mol. Cell. Biol.* **11**, 4796–803
29. McLone, D. G., and Bondareff, W. (1975) *Am. J. Anat.* **142**, 273–294
30. Schmauss, C., McAllister, G., Ohosone, Y., Hardin, J. A., and Lerner, M. R. (1989) *Nucleic Acids Res.* **17**, 1733–1743
31. Zamore, P. D., Patton, J. G., and Green, M. R. (1992) *Nature* **355**, 609–614
32. Shaw, P. J., Highett, M. I., Beven, A. F., and Jordan, E. G. (1995) *EMBO J.* **14**, 2896–2906
33. Vissers, C., Flohil, C., de Jong, A., Dinjens, W. N., and Bosman, F. T. (1996) *Acta Histochem.* **98**, 113–121
34. Ochs, R. L., Stein, T. W. J., Chan, E. K., Ruutu, M., and Tan, E. M. (1996) *Mol. Cell. Biol.* **7**, 1015–1024
35. Sommerville, J. (1986) *Trends Biochem. Sci.* **11**, 438–442
36. Cáceres, J., Stamm, S., Helfman, D. M., and Krainer, A. R. (1994) *Science* **265**, 1706–1709
37. Wang, J., and Manley, J. L. (1995) *RNA* **1**, 335–46
38. Kuo, H.-C., Nasim, F.-U. H., and Grabowski, P. J. (1991) *Science* **251**, 1045–1050
39. Monaghan, K., Van Dyke, D. L., Wiktor, A., Feldman, G. L. (1997) *Am. J. Med. Genet.* **73**, 180–183
40. McKeown, M. (1992) *Annu. Rev. Cell Biol.* **8**, 133–155
41. Bingham, P. M., Chou, T.-B., Mims, I., and Zachar, Z. (1988) *Trends Genet.* **4**, 134–138
42. Pfeffer, U., Fecarotta, E., and Vidali, G. (1995) *Cancer Res.* **55**, 2158–2165
43. De la luna, S., Burden, M. J., Lee, C. W., and Lathangue, N. B. (1996) *J. Cell Sci.* **109**, 2443–2452
44. Grumont, R. J., and Gerondakis, S. (1994) *Proc. Natl. Acad. Sci. U. S. A.* **91**, 4367–4371
45. McLaughlin, S., and Dixon, J. E. (1993) *J. Biol. Chem.* **268**, 6839–6842
46. Borgese, N., D'Arrigo, A., De, S. M., and Pietrini, G. (1993) *FEBS Lett.* **325**, 70–75
47. Snow, B. E., Heng, H. H. Q., Shi, X.-M., Zhou, Y., Du, K., Taub, R., Tsui, L.-C., and McInnes, R. R. (1997) *Genomics* **43**, 165–170
48. Ge, H., Zuo, P., and Manley, J. L. (1991) *Cell* **66**, 373–82
49. Sarkissian, M., Winne, A., and Lafyatis, R. (1996) *J. Biol. Chem.* **271**, 31106–31114
50. Mattox, W., and Baker, B. S. (1991) *Genes Dev.* **5**, 786–796
51. Chou, T. B., Zachar, Z., and Bingham, P. M. (1987) *EMBO J.* **6**, 4095–4104
52. Ochs, R., and Smetana, K. (1989) *Exp. Cell Res.* **184**, 552–557
53. Jordan, E. G., and McGovern, J. H. (1981) *J. Cell Sci.* **52**, 373–389
54. Korb, K., Stokrova, J., Karafiat, V., Dvorakova, M., and Cermakova, V. (1996) *Acta Virol.* **40**, 81–86
55. Iwata, H., Otoshi, T., Takada, N., Murai, T., Tamano, S., Watanabe, T., Katsura, Y., and Fukushima, S. (1995) *Urol. Res.* **23**, 27–32
56. Derenzini, M., Farabegoli, F., and Trerè, D. (1993) *J. Histochem. Cytochem.* **41**, 829–836
57. Mikhaylova, V., and Markov, D. (1994) *Exp. Cell Res.* **212**, 10–21
58. Vilardeil, J., and Warner, J. R. (1997) *Mol. Cell. Biol.* **17**, 1959–1965
59. Hanauer, A. (1983) *Nucleic Acids Res.* **11**, 3503–1516
60. Du, K., Peng, Y., Greenbaum, L. E., Haber, B. A., and Taub, R. (1997) *Mol. Cell. Biol.* **17**, 4096–4104
61. Mayeda, A., and Krainer, A. R. (1992) *Cell* **68**, 365–375
62. Sun, Q., Mayeda, A., Hampson, P. K., Krainer, A. R., and Rottman, F. M. (1993) *Genes Dev.* **7**, 3519–3529
63. Hanamura, A., Cáceres, J. F., Mayeda, A., Franza, B. R., and Krainer, A. R. (1998) *RNA* **4**, 430–444
64. Blencowe, B. J., Issner, R., Nickerson, J., and Sharp, P. (1998) *Genes Dev.* **12**, 996–1009